Chinese Chemical Letters 37 (2026) 112281

Contents lists available at ScienceDirect

Chinese Chemical Letters

journal homepage: www.elsevier.com/locate/cclet

Osmacyclopentatrienyl radicals with a delocalized unpaired electron

Bingjie Fu[a], Yue Zhao[a], Yang Li[b,*], Wenfeng Jiang[a,*], Wei Bai[a,*]

[a] School of Chemistry, Dalian University of Technology, Dalian 116024, China
[b] School of Chemical Engineering, Ocean and Life Sciences, Dalian University of Technology, Panjin 124221, China

ARTICLE INFO

Article history:
Received 8 October 2025
Revised 2 December 2025
Accepted 12 December 2025
Available online 13 December 2025

Keywords:
Antiaromaticity
Osmacyclopentatriene
Osmacyclopentadiene
Radical
Redox reaction

ABSTRACT

Substituted cyclopentadienyl (Cp) radicals, as well as other Cp and fluorenyl-based radicals, exhibit deviations from ideal fivefold D_{5h} symmetric structures due to Jahn-Teller distortion. The unpaired electron is unequally distributed on the five carbons. Herein, we report the metalla-analogs of Cp radicals from one-electron reduction of antiaromatic osmacyclopentatriene complexes. The novel osmacyclopentatrienyl radicals are nonaromatic, with the single unpaired electron delocalized over the entire five-membered osmacycle. Furthermore, these osmacyclopentatrienyl radicals can be oxidized to regenerate osmacyclopentatrienes and reduced to form osmacyclopentadienes. This discovery provides new insights into radical chemistry and organometallic chemistry.

© 2026 Published by Elsevier B.V. on behalf of Chinese Chemical Society and Institute of Materia Medica, Chinese Academy of Medical Sciences.

Radical compounds are one important cornerstones of chemistry. Organic radicals are usually reactive due to their characteristic open-shell electronic structures, and the active unpaired electrons play crucial roles in molecular transformations and functional materials [1,2]. For example, nonaromatic porphyrinoid radicals have been isolated and characterized as the key structures in redox aromatic−antiaromatic switching [3–7]. Recently, Schulz and Haberhauer presented the synthesis of antiaromatic cyclopentadienyl (Cp) cation from the oxidation of Cp radical, which could be reduced to Cp anion [8]. The synthesis and structures of substituted Cp radicals have attracted attention for 100 years since the report of pentaphenyl one (C_5Ph_5) in 1925 by Ziegler and Schnell [9]. Crystallographic studies demonstrate that both symmetrically and asymmetrically substituted Cp radicals, as well as other Cp and fluorenyl-based radicals, exhibit deviations from ideal fivefold D_{5h} symmetry (**A**, Fig. 1) [10–15], while some early works have disorder problems [16,17]. First-principles calculations reveal that Jahn-Teller distortion preferentially stabilizes the C_{2v} symmetric structures (**B** and **C**, Fig. 1) [18,19]. The unpaired electron is not evenly delocalized over the five-membered ring, and the ring shows significant single and double C–C bond alternations [10–15].

The involvement of transition metals in conjugated ring system has shown the potentials for approaching fascinating structures. Recently, Xia group presented the aromatic in-plane [55555] metallo-annulene complexes wherein five aromatic rings share one central Os atom [20]. Both metallaaromatics [21], such as metallabenzene [22], metallabenzyne [23], metallapentalyne [24], spirometallole [25], and rare examples of metalla-antiaromatics [26–31], have been reported. The metalla-analogues of CpH (cyclopentadiene) and Cp^- (cyclopentadienyl anion), such as metallacyclopentadienes [32] and dianion metalloles [33], are well-documented. By contrast, metalla-analog of Cp radicals are less developed, and the unpaired electrons are mainly localized [34–36]. In this work, we report the structure and characterization of the nonaromatic osmacyclopentatrienyl radicals as the first examples of one-electron reduction of antiaromatic metallacycles, which demonstrate unprecedent delocalization of the single unpaired electron (Fig. 1).

Complexes **2** were obtained from the mixture of corresponding antiaromatic osmacyclopentatriene complexes **1** [31], $AgPF_6$ and acetonitrile (MeCN) in dichloromethane (DCM) at 40 °C (Fig. 2a). Single-crystal X-ray diffraction analysis revealed that the cation **2b**$^{2+}$ (the metallacyclic dication of **2**) also contained an osmacyclopentatriene unit (Figs. 2b and c) [31]. For example, the Os=*C* bond lengths in **2b**$^{2+}$ (1.942(6) Å and 1.936(5) Å) are slightly longer than those in complex **1a** (1.927(10) Å and 1.924(11) Å). The C–C single bonds are almost identical (1.488(8) Å and 1.481(8) Å in **2b**$^{2+}$, and 1.489(12) Å and 1.488(12) Å in **1a**), while the C=C double bond (1.354(8) Å) of **2b**$^{2+}$ is much shorter than that of **1a** (1.377(13) Å) [31]. The NMR data of **2b** are consistent with its solid structure. For instance, its $^{31}P\{^1H\}$ NMR spectrum shows a singlet at −7.7 ppm, confirming the two identical *trans*-oriented PPh_3, and the septet at −144.3 ppm is from the counterion PF_6^-. In the ^1H NMR spectrum, the signal of MeCN appears at 2.54 ppm, and the other resonances are all in the range of 7.22–7.96 ppm with well-

* Corresponding authors.
E-mail addresses: chyangli@dlut.edu.cn (Y. Li), jiangwf@dlut.edu.cn (W. Jiang), baiwei@dlut.edu.cn (W. Bai).

https://doi.org/10.1016/j.cclet.2025.112281
1001-8417/© 2026 Published by Elsevier B.V. on behalf of Chinese Chemical Society and Institute of Materia Medica, Chinese Academy of Medical Sciences.

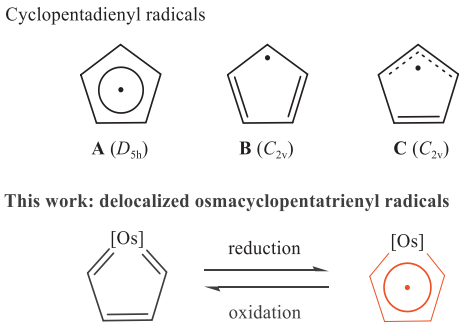


Fig. 1. Five-membered cyclic C_5 and MC_4 radical compounds.

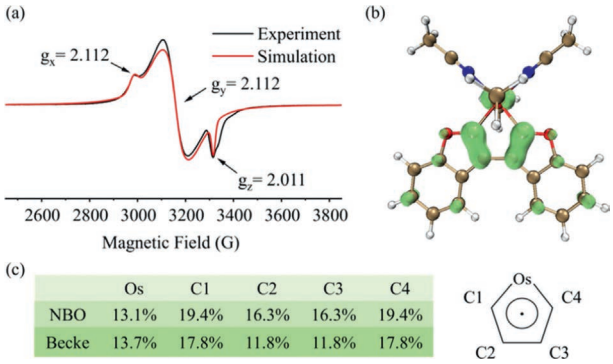


Fig. 3. (a) The EPR spectrum of **3a** at 110 K in solid state. (b) The spin density of **3′**. (c) The spin population of **3′** was calculated using NBO and Becke methods.

resolved coupling patterns, which is indicative of a diamagnetic molecule and implies a good symmetry for **2b**$^{2+}$. The Os=C signal of **2b**$^{2+}$ is found at 237.8 ppm as a triplet (J(PC) = 10.1 Hz) in the $^{13}C\{^1H\}$ NMR spectrum, which is downfield-shifted (by 8.8 ppm) compared with that of **1b**. Complex **2a** has similar NMR spectra (Figs. S22-S24 in Supporting information), and **2a** and **2b** are also characterized by the high-resolution mass spectrometry (HRMS, Figs. S34 and 35 in Supporting information), as well as elemental analysis (EA). Generally, the NMR data and structural parameters suggest that complexes **2** have similar polycyclic structures as **1**. Meanwhile, their electronic structures and aromatic property are comparable, revealed by aftermentioned theoretical studies.

Upon exposure to reducing agents (CuI, Zn, or $NaBH_4$), the reddish solution of complexes **2** underwent a rapid color change to green. Osmacyclopentatrienyl radicals **3** were precipitated out after counterion exchange with $NaBPh_4$ (Fig. 2a). Complexes **3** were paramagnetic, and single-crystal X-ray diffraction analysis confirmed the structure of **3b** As shown in Figs. 2b and c, **3b**$^{\cdot+}$ (the metallacyclic cation of **3b**) has a much more delocalized five-membered OsC_5 ring. The Os–C bonds (1.998(4) Å and 1.995(4) Å) of **3b**$^{\cdot+}$ are longer than those of **2b**$^{2+}$ and **1a**, while the C–C bond lengths in the osmacycle (1.421(5) Å, 1.423(5) Å, and 1.399(5) Å) demonstrate a trend toward equalization. These Os-C and C–C bond distances of the OsC_5 ring in **3b**$^{\cdot+}$ obviously fall between those of characteristic osmacyclopentatriene **2b**$^{2+}$ and aftermentioned osmacyclopentadiene **4b**. Electronic paramagnetic resonance (EPR) spectroscopy was employed to characterize radicals **3** (Fig. 3a and Fig. S1a in Supporting information). Simulations yielded $g_{x,y,z}$ = 2.231, 2.112, 2.011 of **3a**, and $g_{x,y,z}$ = 2.278, 2.115, 2.012 of **3b**, indicating that the unpaired electron occupied d_{xz} or d_{yz} orbital of the Os metal center (Fig. S1b in Supporting information), and the d_{xz} orbital contributed to the molecular π

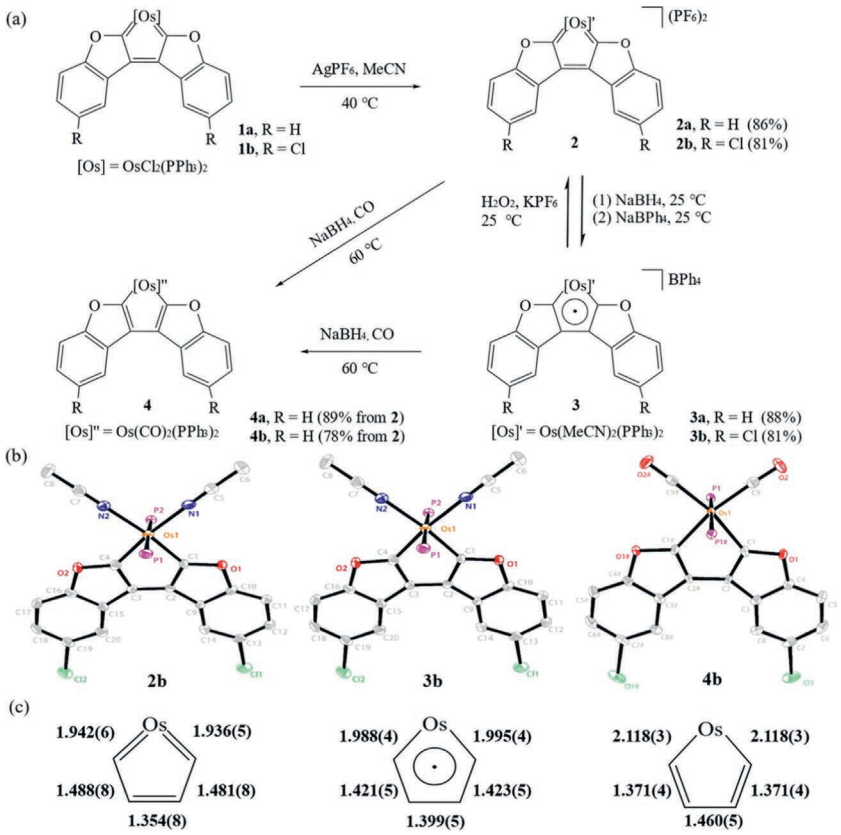


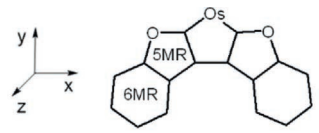
Fig. 2. (a) Formation of complexes **2**, **3** and **4**. (b) ORTEP drawing of **2b**$^{2+}$, **3b**$^{\cdot+}$ and **4b** (symmetry code#: 1-X, +Y, 3/2-Z) with thermal ellipsoids set 50% probability (phenyl groups of PPh_3 and hydrogen atoms are omitted for clarity). (c) Selected bond distances (Å) in **2b**$^{2+}$, **3b**$^{\cdot+}$ and **4b**.

orbitals (aftermentioned theoretical studies). Their EPR spectra in DCM solution at room temperature were similar (Fig. S2 in Supporting information), showing only the signals of metal radical. The structural formula and purity of **3** have been confirmed by HRMS (Figs. S36 and S37 in Supporting information) and EA, respectively. When complexes **3** were treated with KPF_6 and H_2O_2 (5 wt%), oxidation occurred with the regeneration of **2** (Fig. 2a).

Density functional theory (DFT) calculations were performed on model complex **3′** (simplified by replacing PPh_3 with PH_3) using the UB3LYP-D3BJ//def2-TZVP/6–311 G(2d,p) level of theory [37–40]. The optimized structure of **3′** accurately reproduced the key features of **3b**$^{\cdot+}$ (Fig. S5 in Supporting information). The spin density analysis [41,42] showed that the single unpaired electron of **3′** is predominantly delocalized on the five atoms of the OsC_4 unit (Fig. 3b). Spin population analysis was further carried out using Becke method [43], indicating nearly even distribution over the five atoms that the Os occupied 13.7 % and the four carbons occupied 17.8 % or 11.8 % (Fig. 3c). NBO method [44,45] showed a consistent result with 13.1 % to 19.4 % spin population (Fig. 3c). The spin distributions of the remaining atoms were presented in Fig. S6 (Supporting information). The hyperfine splitting of C_4 unit was unresolved in EPR spectra, probably due to the broad linewidths of Os signal [46–48]. For comparison, we optimized the two types of C_{2v} symmetric substituted cyclopentadienyl radicals **Cp-B** and **Cp-C** reported in the literature (structures **B** and **C**, Fig. 1) [12], and calculated their spin density and spin population analysis by Becke method. As shown in Fig. S7 (Supporting information), the single unpaired electron of **Cp-B** is predominantly distributed on C1 (35.7 %), and C3 (23.0 %) and C4 (20.5 %), while the single unpaired electron of **Cp-C** is predominantly distributed on the terminal carbons of the vinylic radical (C2 30.2 %, C5 29.0 %), consistent with the reported results. The delocalization of the single unpaired electron over the five-membered osmacycle in **3** is quite unique, in sharp contrast to previously reported aromatic [34,49] and non-aromatic [50] conjugated metallacycles containing single unpaired electron, which is mainly localized on the metal center.

It was found that the addition of a large excess of $NaBH_4$ could further reduce complexes **3** with a color change from green to pale yellow. We investigated the reactions and complexes **4** were obtained from the reactions of **3** (or **2**) with $NaBH_4$ under carbon monoxide atmosphere (Fig. 2a), and their structures were determined by single-crystal X-ray diffraction. As shown in Figs. 2b and c, Figs. S20 and S21 (Supporting information), both **4a** and **4b** contain an osmacyclopentadiene unit and the Os center is coordinated with two equatorial CO and two axial PPh_3 ligands. The Os-C bond lengths (2.107(7) Å and 2.137(7) Å for **4a**, 2.118(3) Å for **4b**) are in the range of the Os-C single bonds (1.977(2)-2.183(7) Å) in monocyclic osmacyclopentadiene complexes [51–54]. The C–C bonds (1.354(10) Å, 1.362(9) Å, and 1.453(10) Å for **4a**, 1.371(4) Å and 1.460(5) Å for **4b**) of the osmacycles show significant single and double bond alternations. The NMR data supports this solid structure. The Os-C=C of **4b** is found at 180.2 ppm as a triplet (J(PC) = 10.1 Hz) in the $^{13}C\{^1H\}$ NMR spectrum, which is remarkably upfield-shifted compared with those of **2b** and **1b**. The *C*O signal is found at 184.9 ppm (t, J(PC) = 10.1 Hz). All the proton signals appear in the aromatic region of 7.53–6.75 ppm in the ^1H NMR spectrum. The $^{31}P\{^1H\}$ NMR spectrum displays a singlet at −1.8 ppm. Complex **4a** shows similar NMR spectra (Figs. S28-S30 in Supporting information), and they are also characterized by HRMS (Figs. S38 and S39 in Supporting information) and EA. The solids of complexes **2**, **3**, and **4** can be stored at ambient condition for three months without obvious change.

The nucleus-independent chemical shifts (NICS) [55–58] were calculated to evaluate the aromatic property of these metallapolycycles in model complexes **2′**, **3′**, and **4′**, which are simplified from **2b**$^{2+}$, **3b**$^{\cdot+}$, and **4b**, respectively. The NICS(1)$_{zz}$ values of the fused benzene units (**6MR**) are all negative (Fig. 4), suggesting that they are aromatic. While the NICS(1)$_{zz}$ value of the osmacyclopentatriene ring of **2′** is 18.8 ppm, indicating its antiaromaticity like complex **1** [31]. Whereas the osmacyclopentatrienyl radical unit of **3′** and the osmacyclopentadiene unit of **4′** are nonaromatic as their NICS(1)$_{zz}$ values are 7.4 ppm and 3.0 ppm, respectively. From **2′** to **4′**, the oxa-rings (**5MR**) turn from nonaromatic (NICS(1)$_{zz}$ = 4.8 ppm for **2′**) to nonaromatic (NICS(1)$_{zz}$ = −7.1 ppm for **3′**), and aromatic (NICS(1)$_{zz}$ = −18.2 ppm for **4′**). This transformation aligns with the changes in structural parameters (Fig. 2c and Fig. S5), especially the C–C bonds shared between the osmacycle and **5MR**. Isodesmic reaction energies [59–61] were calculated by breaking the C=C bond in the osmacyclopentatriene unit of **2′**, and the negative values (−15.9 kcal/mol and −8.9 kcal/mol, Fig. S13 in Supporting information) also supported its antiaromaticity as the transformations of the antiaromatic ring to acyclic or non-conjugated structures were thermodynamically favorable. Furthermore, the anisotropy of the induced current density (AICD) study [62,63] was performed on **2′**, **3′** and **4′** (Figs. S10-S12 in Supporting information). Clockwisely diatropic ring currents induced by an external magnetic field were observed in all **6MR** and the **5MR** of **4′**, confirming their aromaticity. The antiaromatic osmacyclopentatriene unit of **2′** demonstrated counterclockwisely paratropic ring currents, while there is no regular current on the other rings. The gauge including magnetically induced current (GIMIC) [64–66] was also studied (Figs. S14-S16 in Supporting information). The antiaromatic osmacyclopentatriene unit of **2′** showed counterclockwisely paratropic ring currents with the negative current intensity passing through the integral plane (between −3.45 and −4.55 nÅ/T), while the nonaromatic osmacyclopentatrienyl radical unit of **3′** and the osmacyclopentadiene unit of **4′** exhibited no obviously paratropic or diatropic ring currents.



NICS(1)$_{zz}$	osmacycle	5MR	6MR
2'	18.8	4.8	-18.5
3'	7.4	-7.1	-23.6
4'	3.0	-18.2	-27.7

Fig. 4. The computed NICS(1)$_{zz}$ values (in ppm) of **2′**, **3′** and **4′**.

Fig. 5 depicts the key frontier molecular orbitals of complexes **2**, **3**, and **4**, in which the metal center and ligands form an octahedral coordination geometry from the perspective of crystal field theory. In **3**, the SOMO (singly occupied molecular orbital) is predominantly composed of the π molecular orbitals located on carbons of the OsC_4 unit and the non-bonding orbitals with t_{2g} symmetry originating from the metal d_{xz} orbital. This composition aligns well with the EPR and the spin density analysis results presented in Fig. 3. The SOMO-1 is mainly constituted by the metal d_{yz} orbital, and it retains a non-bonding nature with t_{2g} symmetry. The interaction between the metal d_{z^2} orbital and the ligand SALC (Symmetry Adapted Linear Combination) orbitals generates the LUMO of **3**, which results in metal-centered σ^*-antibonding MOs (possessing e_g symmetry). The LUMO+1, LUMO, and HOMO of **2** exhibit similar orbital patterns to the LUMO, SOMO and SOMO-1 of **3**, and LUMO, HOMO and HOMO-1 of **4** (Fig. 5). The osmacyclopentatriene ring of **2** can be identified as a 5-center 6-electron (5c-6e) Craig-Möbius antiaromatic system with three occupied π molecular orbitals (π-MOs, HOMO, HOMO-16 and HOMO-17, Fig. S17 in Supporting information), HOMO-16 of which participated in p_π–d_π interaction in

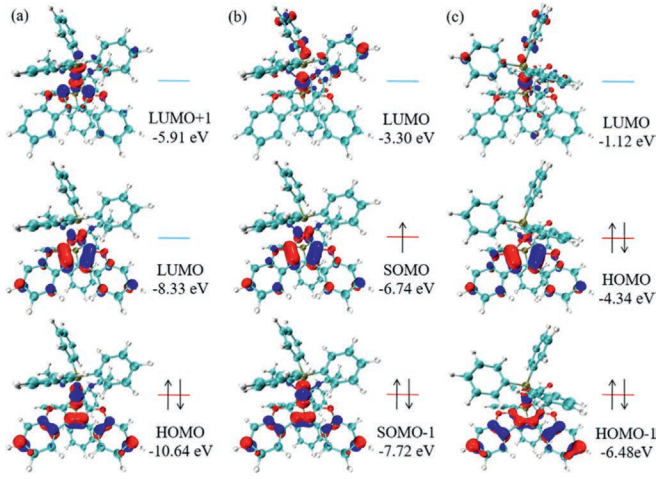


Fig. 5. Key frontier molecular orbitals of (a) **2**, (b) **3**, (c) and **4** (isovalue of 0.05 a.u.).

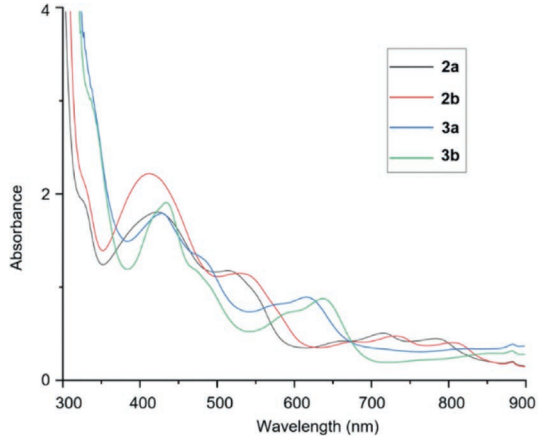


Fig. 6. UV–vis absorption spectra of complexes **2** and **3** (9.0×10^{-5} mol/L) measured in DCM at room temperature.

the π-MOs involved the phase shift in the osmium center [27,31]. Since the SOMO in **3** has the π-MO character, the presence of delocalized single unpaired electron results in the nonaromaticity of the osmacyclopentatrienyl radical.

The ultraviolet-visible (UV–vis) absorption spectra of **2**–**4** were measured. As shown in Fig. 6, their maximum absorptions are all around 410–440 nm in the region of 300–800 nm (**2a**, 424 nm, $\log\varepsilon = 6.500\ M^{-1}\ cm^{-1}$; **2b**, 412 nm, $\log\varepsilon = 6.583\ M^{-1}\ cm^{-1}$; **3a**, 430 nm, $\log\varepsilon = 6.502\ M^{-1}\ cm^{-1}$; **3b**, 437 nm, $\log\varepsilon = 6.516\ M^{-1}\ cm^{-1}$; where ε is the molar extinction coefficient), which are attributed to metal-to-ligand charge transfer (MLCT) transitions involving the osmium center and the conjugated π-system of the ligand. There are also distinct absorptions at around 610–640 nm of **3** (**3a**, 615 nm, $\log\varepsilon = 6.221\ M^{-1}\ cm^{-1}$, **3b**, 639 nm, $\log\varepsilon = 6.219\ M^{-1}\ cm^{-1}$), which likely arise from intra-ligand π–π^* transitions or low-energy D-d transitions associated with the open-shell Os configuration. The extended absorption tails of **2** beyond 700–800 nm are consistent with their antiaromaticity [27,31]. Unsurprisingly, the pale-yellow complexes **4** have no obvious absorptions in the region. In addition, time-dependent density functional theory (TD-DFT) calculations were carried out on model $\mathbf{2a}^{2+}$ and $\mathbf{3a}^{\cdot+}$ in DCM medium [67,68]. As shown in Table S1, and Figs. S8 and S9 (Supporting information), the simulated results agree well with the experimental data.

Cyclic voltammetry (CV) was performed to study the electronic properties of **2a**, **3a** and **4a**. The measured onset reduction and oxidation potentials for **2a**, **3a** and **4a** were −1.35/0.52 V, −0.81/0.64 V and −1.45/0.78 V, respectively (Fig. S3 in Supporting information). The results also show that **2** can be stepwisely reduced with two reduction peaks, while **3** can undergo another reduction step.

To investigate the oxidation states of metal centers in these structures, X-ray photoelectron spectroscopy (XPS) measurements were performed on **2a**, **3a**, and **4a** (Fig. S4 in Supporting information). The results revealed that the binding energies of the Os $4f_{5/2}$ and $4f_{7/2}$ orbitals in **2a** were 53.8 eV and 51.1 eV, respectively, while those in **3a** were 52.6 eV and 50.1 eV. These values are consistent with the previously reported data for Os(IV) and Os(III) [69,70]. For **4a**, the binding energies of the Os $4f_{5/2}$ and $4f_{7/2}$ orbitals were determined to be 53.5 eV and 50.8 eV, respectively, which agreed with the results of Os(II) with CO ligands in the literature [71]. It is noted that the ligands can significantly affect the binding energies of metal centers [72–74].

In conclusion, novel osmacyclopentatrienyl radicals **3** with a delocalized unpaired electron in the OsC_4 ring are obtained from the reduction of antiaromatic osmacyclopentatrienes **2**. The unique electronic structure of **3** has been characterized by EPR, spin density, spin population and MO analysis. Complexes **3**, as well as **2**, can be further reduced to nonaromatic osmacyclopentadienes **4** under CO atmosphere. The osmacyclopentatrienyl radicals show similar one-electron redox reactivity as Cp radicals, while they have differences in the unpaired electron distribution. This study provides new insights into radical chemistry and organometallic chemistry.

CRediT authorship contribution statement

Bingjie Fu: Writing – original draft, Investigation, Formal analysis. **Yue Zhao:** Investigation, Formal analysis. **Yang Li:** Writing – review & editing, Supervision. **Wenfeng Jiang:** Supervision, Funding acquisition. **Wei Bai:** Writing – review & editing, Writing – original draft, Supervision, Funding acquisition, Formal analysis, Conceptualization.

Declaration of competing interest

The authors declare that they have no known competing financial interests or personal relationships that could have appeared to influence the work reported in this paper.

Acknowledgments

This research is supported by the National Natural Science Foundation of China (No. 22001030) and the Liaoning Provincial Natural Science Foundation (No. 2025-MS-001). The authors acknowledge Dr. Guang Zeng from the Dalian Institute of Chemical Physics (Chinese Academy of Sciences) for his help on EPR study, and the support from DUT IAC and "Supercomputing Center of Dalian University of Technology".

Supplementary materials

Supplementary material associated with this article can be found, in the online version, at doi:10.1016/j.cclet.2025.112281.

References

[1] R.G. Hicks, Stable Radicals: Fundamental and Applied Aspects of Odd-electron Compounds, Wiley-Blackwell, New York, 2010.
[2] R.G. Hicks, Org. Biomol. Chem. 5 (2007) 1321–1388.
[3] H. Gao, F. Wu, Y. Zhao, et al., J. Am. Chem. Soc. 144 (2022) 3458–3467.
[4] T. Sarma, G. Kim, S. Sen, Y. Cha, Z. Duan, J. Am. Chem. Soc. 140 (2018) 12111–12119.
[5] T. Satoh, M. Minoura, H. Nakano, et al., Angew. Chem. Int. Ed. 55 (2016) 2235–2238.

[6] T.Y. Gopalakrishna, J.S. Reddy, V.G. Anand, Angew. Chem. Int. Ed. 53 (2014) 10984–10987.
[7] M. Ishida, S. Kim, C. Preihs, et al., Nat. Chem. 5 (2012) 15–20.
[8] Y. Schulte, C. Wölper, S.M. Rupf, et al., Nat. Chem. 16 (2024) 651–657.
[9] K. Ziegler, B. Schnell, Justus Liebigs Ann. Chem. 445 (1925) 266–282.
[10] T. Kitagawa, K. Ogawa, K. Komatsu, J. Am. Chem. Soc. 126 (2004) 9930–9931.
[11] P.R. Nimax, F. Zoller, T. Blockhaus, et al., New J. Chem. 44 (2020) 72–78.
[12] Y. Schulte, B.L. Geoghegan, C. Helling, et al., J. Am. Chem. Soc. 143 (2021) 12658–12664.
[13] Z. Gong, Q. Xiang, K. Li, et al., Chin. J. Chem. 40 (2022) 2525–2530.
[14] Y. Tian, K. Uchida, H. Kurata, et al., J. Am. Chem. Soc. 136 (2014) 12784–12793.
[15] K. Kato, A. Osuka, Angew. Chem. Int. Ed. 58 (2019) 8978–8986.
[16] H. Sitzmann, R. Boese, Angew. Chem. Int. Ed. 30 (1991) 971–973.
[17] C. Janiak, R. Weimann, F. Görlitz, Organometallics 16 (1997) 4933–4936.
[18] L.C. Snyder, J. Chem. Phys. 33 (1960) 619–621.
[19] L.C. Snyder, J. Phys. Chem. 66 (1962) 2299–2306.
[20] B. Xu, D. Chen, K. Ruan, et al., Nature 641 (2025) 106–111.
[21] D. Chen, Y. Hua, H. Xia, Chem. Rev. 120 (2020) 12994–13086.
[22] G.P. Elliott, W.R. Roper, J.M. Waters, J. Chem. Soc., Chem. Commun. (1982) 811–813.
[23] T.B. Wen, Z.Y. Zhou, G. Jia, Angew. Chem. Int. Ed. 40 (2001) 1951–1954.
[24] C. Zhu, S. Li, M. Luo, et al., Nat. Chem. 5 (2013) 698–703.
[25] Y. Zhang, J. Wei, Y. Chi, et al., J. Am. Chem. Soc. 139 (2017) 5039–5042.
[26] K. Zhuo, Y. Liu, K. Ruan, et al., Nat. Synt. 2 (2022) 67–75.
[27] L. Chen, L. Lin, A.R. Nath, et al., Proc. Natl. Acad. Sci. U. S. A. 120 (2023) e2215900120.
[28] Q. Li, Y. Hua, C. Tang, et al., J. Am. Chem. Soc. 145 (2023) 7580–7591.
[29] K. Miwa, T. Yokota, Q. Wang, et al., J. Am. Chem. Soc. 146 (2024) 1396–1402.
[30] Y. He, Y. Zhu, M. Luo, et al., Chin. Chem. Lett. 36 (2025) 110463.
[31] B. Fu, Y. Wang, Y. Zhao, et al., J. Am. Chem. Soc. 146 (2024) 30790–30795.
[32] W. Ma, C. Yu, T. Chen, et al., Chem. Soc. Rev. 46 (2017) 1160–1192.
[33] J. Wei, W. Zhang, Z. Xi, Chem. Sci. 9 (2018) 560–568.
[34] Z. Huang, Y. Zhang, W. Zhang, et al., Nat. Commun. 12 (2021) 1319.
[35] X. Zhang, J. Wang, L. Xu, et al., CCS Chem. 4 (2022) 3832–3841.
[36] X. Jin, J. Wang, X. Yang, et al., Inorg. Chem. 62 (2023) 19323–19331.
[37] A.D. Becke, J. Chem. Phys. 98 (1993) 5648–5652.
[38] B. Miehlich, A. Savin, H. Stoll, et al., Chem. Phys. Lett. 157 (1989) 200–206.
[39] C. Lee, W. Yang, R.G. Parr, Phys. Rev. B 37 (1988) 785–789.
[40] P.J. Hay, W.R. Wadt, J. Chem. Phys. 82 (1985) 299–310.
[41] T. Lu, F. Chen, J. Comput. Chem. 33 (2012) 580–592.
[42] T. Lu, J. Chem. Phys. 161 (2024) 082503.
[43] A.D. Becke, J. Chem. Phys. 88 (1988) 2547–2553.
[44] L.W. DeVetter, E. Beaver, J. Colquhoun, et al., Eur. J. Hortic. Sci. 81 (2016) 321–326.
[45] K.B. Wiberg, Tetrahedron 24 (1968) 1083–1096.
[46] M. Zrfar, A. Ahmad, S. Saha, et al., Chem. Sci. 13 (2022) 8567–8575.
[47] S. Ye, B. Sarkar, C. Duboc, J. Fiedler, W. Kaim, Inorg. Chem. 44 (2005) 2843–2847.
[48] W. Kaim, Coord. Chem. Rev. 76 (1987) 187–235.
[49] W. Bai, L. Li, Y. Fu, et al., Dalton Trans. 52 (2023) 9731–9736.
[50] X. Yang, Q. Deng, S. Liu, et al., Inorg. Chem. Front. 12 (2025) 3909–3918.
[51] T. Wang, H. Zhang, F. Han, et al., Chem. Eur. J. 19 (2013) 10982–10991.
[52] J. Chen, Z. Huang, Y. Hua, et al., Organometallics 34 (2014) 340–347.
[53] T. Wang, F. Han, H. Huang, et al., Sci. Rep. 5 (2015) 9584.
[54] C. Zhu, J. Zhu, X. Zhou, et al., Angew. Chem. Int. Ed. 57 (2018) 3154–3157.
[55] P.V.R. Schleyer, C. Maerker, A. Dransfeld, et al., J. Am. Chem. Soc. 118 (1996) 6317–6318.
[56] P.V.R. Schleyer, H. Jiao, N.J.R.V. Hommes, et al., J. Am. Chem. Soc. 119 (1997) 12669–12670.
[57] Z. Chen, C.S. Wannere, C. Corminboeuf, et al., Chem. Rev. 105 (2005) 3842–3888.
[58] H. Fallah-Bagher-Shaidaei, C.S. Wannere, C. Corminboeuf, et al., Org. Lett. 8 (2006) 863–866.
[59] R. Herges, D. Geuenich, J. Phys. Chem. A 105 (2001) 3214–3220.
[60] D. Geuenich, K. Hess, F. Köhler, et al., Chem. Rev. 105 (2005) 3758–3772.
[61] W.J. Hehre, R. Ditchfield, L. Radom, et al., J. Am. Chem. Soc. 92 (1970) 4796–4801.
[62] A.A. Deniz, K.S. Peters, G.J. Snyder, Science 286 (1999) 1119–1122.
[63] S.E. Wheeler, K.N. Houk, P.V.R. Schleyer, et al., J. Am. Chem. Soc. 131 (2009) 2547–2560.
[64] H. Fliegl, S. Taubert, O. Lehtonen, et al., Phys. Chem. Chem. Phys. 13 (2011) 20500–20518.
[65] D. Sundholm, H. Fliegl, R.J.F. Berger, WIREs Comput. Mol. Sci. 6 (2016) 639–678.
[66] Z. Badri, C. Foroutan-Nejad, Nat. Rev. Chem. 8 (2024) 551–560.
[67] C. Adamo, D. Jacquemin, Chem. Soc. Rev. 42 (2013) 845–856.
[68] M. Huix-Rotllant, A. Nikiforov, W. Thiel, et al., Description of Conical Intersections With Density Functional Methods., Topics in Current Chemistry, Springer International Publishing, 2015, pp. 445–476.
[69] D.D. Sarma, C.N.R. Rao, J. Electron Spectrosc. Relat. Phenom. 20 (1980) 25–45.
[70] S. Gayen, F. Assanar, S. Shyamal, D.P. Dorairaj, S. Ghosh, Chem. Sci. 15 (2024) 15913–15924.
[71] A.R. Siedle, R.A. Newmark, G.A. Korba, L.H. Pignolet, Paul D. Boyle, Inorg. Chem. 27 (1988) 1593–1598.
[72] X. Fu, Y. Wang, N. Wu, et al., J. Colloid Interface Sci. 243 (2001) 326–330.
[73] M. Giuliano, J. Electron. Spectrosc. Relat. Phenom. 95 (1998) 95–144.
[74] R. Zanoni, V. Carinci, Raja H. Abu-Samn, R. Psaro, C. Dossi, J. Mol. Struct. 131 (1985) 363–369.